Mon. Not. R. Astron. Soc. **000**, 1–11 (2014) Printed 18 December 2014 (MN LATEX style file v2.2)

The critical accretion luminosity for magnetized neutron stars

Alexander A. Mushtukov,[1,2⋆] Valery F. Suleimanov,[3,4] Sergey S. Tsygankov[1,5] and Juri Poutanen[1]

[1] *Tuorla Observatory, Department of Physics and Astronomy, University of Turku, Väisäläntie 20, FI-21500 Piikkiö, Finland*
[2] *Pulkovo Observatory of Russian Academy of Sciences, Saint-Petersburg 196140, Russia*
[3] *Institut für Astronomie und Astrophysik, Kepler Center for Astro and Particle Physics, Universität Tübingen, Sand 1, D-72076 Tübingen, Germany*
[4] *Kazan (Volga region) Federal University, Kremlevskaja str., 18, Kazan 420008, Russia*
[5] *Finnish Centre for Astronomy with ESO (FINCA), University of Turku, Väisäläntie 20, FI-21500 Piikkiö, Finland*

arXiv:1409.6457v2 [astro-ph.HE] 17 Dec 2014

18 December 2014

ABSTRACT

The accretion flow around X-ray pulsars with a strong magnetic field is funnelled by the field to relatively small regions close to the magnetic poles of the neutron star (NS), the hotspots. During strong outbursts regularly observed from some X-ray pulsars, the X-ray luminosity can be so high, that the emerging radiation is able to stop the accreting matter above the surface via radiation-dominated shock, and the accretion column begins to rise. This border luminosity is usually called the "critical luminosity". Here we calculate the critical luminosity as a function of the NS magnetic field strength B using exact Compton scattering cross section in strong magnetic field. Influence of the resonant scattering and photon polarization is taken into account for the first time. We show that the critical luminosity is not a monotonic function of the B-field. It reaches a minimum of a few 10^{36} erg s^{-1} when the cyclotron energy is about 10 keV and a considerable amount of photons from a hotspot have energy close to the cyclotron resonance. For small B, this luminosity is about 10^{37} erg s^{-1}, nearly independent of the parameters. It grows for the B-field in excess of 10^{12} G because of the drop in the effective cross-section of interaction below the cyclotron energy. We investigate how different types of the accretion flow and geometries of the accretion channel affect the results and demonstrate that the general behaviour of the critical luminosity on B-field is very robust. The obtained results are shown to be in a good agreement with the available observational data and provide a necessary ground for the interpretation of upcoming high quality data from the currently operating and planned X-ray telescopes.

Key words: scattering – stars: neutron – pulsars: general – X-rays: binaries

1 INTRODUCTION

The strong magnetic field (B-field) with the strength as high as 10^{12}–10^{13} G in X-ray pulsars (XRPs) strongly affects the accretion process to the neutron star (NS). Namely, at some distance from the NS, called magnetospheric radius, the magnetic pressure balances the ram pressure of the infalling gas. At this point, plasma cannot move across the magnetic field lines any more, and hence funnelled to the relatively small regions on the NS surface close to the magnetic poles, the hotspots, where releases its kinetic energy in X-rays. Compactness of the hotspots (whose area could as small as 10^{-5}–10^{-4} of the total NS surface) in combination with the high mass accretion rate (occurring for example during giant type II outbursts observed from XRPs with Be companions) lead to a strong radiation pressure force that is able to stop the infalling matter above the NS surface. This happens at the so called *critical* luminosity (Basko & Sunyaev 1976). With the further increase of the mass accretion rate, and hence the luminosity, the accretion column starts to rise above the hotspot. Therefore, the critical luminosity divides two regimes of accretion onto a NS with strong magnetic field. Below it, plasma reaches the NS surface heating it up via Coulomb collisions (Zel'dovich & Shakura 1969). At higher luminosities, when the accretion column is expected to rise, the accreted matter is decelerated in the radiation-dominated shock on top of the column (Basko & Sunyaev 1976).

⋆ E-mail: al.mushtukov@gmail.com

Observational manifestation of dependence of the accretion column height on the XRP luminosity is an anti-correlation of the cyclotron absorption line energy with the observed source flux (Tsygankov et al. 2006; Tsygankov, Lutovinov, & Serber 2010). Such cyclotron absorption features (sometimes with higher harmonics) observed in the energy spectra of XRPs (Coburn et al. 2002; Filippova et al. 2005; Caballero & Wilms 2012) provide a standard method to estimate the magnetic field strength (Gnedin & Sunyaev 1974). Qualitative explanation of a negative correlation of the cyclotron energy with luminosity in bright pulsars has been proposed by different authors (Mihara, Makishima, & Nagase 2004; Poutanen et al. 2013; Nishimura 2014). Interestingly, in the low-luminosity XRPs, a positive correlation of the cyclotron line energy with flux was observed (Staubert et al. 2007; Yamamoto et al. 2011; Klochkov et al. 2012). The models explaining this behaviour assume that in this case the pulsar luminosity is below the critical one (Staubert et al. 2007; Mukherjee, Bhattacharya, & Mignone 2013).

Different behaviour of the "cyclotron energy – luminosity" dependence gives a possibility to estimate the value of the luminosity from observations. The luminosity where the positive correlation is changed by the negative one can be associated with the critical luminosity, where the radiation pressure is strong enough to stop the infalling matter. Measuring the value of the critical luminosity is extremely important because it contains valuable information about interaction of radiation with matter in strong B-field.

The value of the critical luminosity is defined by processes which provide radiation pressure. In a case of strongly magnetized NSs, it is mainly Compton scattering (see Section 2). Because the scattering cross-section in strong magnetic field has a rather complicated behaviour (it depends strongly on photon energy, polarization state and the B-field strength, and includes a number of resonances, see Herold, Ruder, & Wunner 1982; Daugherty & Harding 1986; Harding & Daugherty 1991), calculation of the effective cross-section becomes a key problem.

Following the ideas already discussed in the literature (Gnedin & Sunyaev 1973; Mitrofanov & Pavlov 1982), we compute here the critical luminosity accurately accounting for the first time for the influence of resonances in the Compton scattering cross-section, polarization, and the geometry of the accretion flow. We base our calculations on the physical model described by Basko & Sunyaev (1976) where it is shown that the critical luminosity is not associated with the standard Eddington limit, but should also account for braking the plasma infalling with high velocity above the NS surface.[1] Finally, we compare the obtained theoretical dependences of the critical luminosity on the magnetic field strength with the available observational data.

[1] A previous attempt to compute the critical luminosity by Becker et al. (2012) was based on an erroneous assumption that the critical luminosity is associated with the Eddington limit. They have also neglected the possibility of mixed polarization states and assumed that all photons are below the cyclotron energy neglecting thus strong resonances in the cross-section.

2 BASIC RELATIONS

The accretion column in XRPs arises as soon as the radiation pressure force $g_{\rm R}$ becomes high enough to stop the infalling matter from the free-fall velocity down to zero above the NS surface (Basko & Sunyaev 1975). The necessary radiation pressure force is significantly larger than the Eddington radiation pressure force which balances the NS gravitational acceleration

$$g_{\rm Edd} = \frac{GM}{R^2}(1-u)^{-1/2}. \quad (1)$$

Here M and R are NS mass and radius, $u = R_{\rm S}/R$ is the compactness parameter and $R_{\rm S} = 2GM/c^2$ is the NS Schwarzschild radius.

The radiative acceleration $g_{\rm R}$ necessary to stop the infalling matter can be evaluated with a simple approach (Basko & Sunyaev 1975). Let us assume that the accreting matter heats NS surface and forms a bright axisymmetric spot of diameter d ($d \ll R$) which radiates all the kinetic energy. Ignoring any relativistic effects, one can find out the radiative acceleration at the distance z above the spot:

$$g_{\rm R} \approx \frac{2\pi}{c}\int_0^\infty dE \int_{\mu_0(z)}^1 \kappa(B,\mu,E)\, I(\mu,E)\, \mu\, d\mu, \quad (2)$$

where κ is the opacity for the interaction process, $\mu = \cos\theta$ with θ being the angle measured from the radial direction and $\mu_0(z) = 1/\sqrt{1+(d/2z)^2}$ is defined by the angular size of the hotspot as seen from a given point above the NS surface (see Fig. 1). Assuming isotropic specific intensity $I(\mu) \approx F/\pi$, where $F = L/2S$ is the hotspot bolometric flux, $S \approx \pi d^2/4$ is the spot area and L is the total XRP luminosity, one gets

$$g_{\rm R} \approx \frac{\kappa_{\rm eff}}{c} F\left[1-\mu_0^2(z)\right] \approx \frac{\kappa_{\rm eff}}{c}\frac{L}{2S}\frac{d^2}{d^2+4z^2}, \quad (3)$$

where $\kappa_{\rm eff}$ is the effective opacity. The last term in equation (3) drops rapidly with the distance from the surface at $z > d/2$ (Basko & Sunyaev 1975) and $g_{\rm R} \propto (d/z)^2$. As a result the radiation pressure decelerates the matter effectively only within a layer $0 < z \lesssim d/2$, where the radiation force is almost constant

$$g_{\rm R} \approx \frac{\kappa_{\rm eff}}{c} F. \quad (4)$$

Taking into account the characteristic braking length $\sim d/2$ and assuming that the velocity of matter has to drop from the free falling velocity $v_{\rm ff} \approx c\sqrt{R_{\rm S}/R}$ at $z \approx d/2$ down to zero at the surface, we can estimate the necessary deceleration:

$$g \approx \frac{v_{\rm ff}}{t_{\rm ff}} \approx \frac{v_{\rm ff}^2}{d}, \quad (5)$$

where $t_{\rm ff}$ is a characteristic free-fall time. Therefore, using an equality $g_{\rm R} = g$, we can find a hotspot flux F^*, which is sufficient to stop matter by the radiation pressure

$$F^* \approx \frac{c}{\kappa_{\rm eff}}\frac{v_{\rm ff}^2}{d}. \quad (6)$$

Corresponding critical luminosity for a circular spot is then (Basko & Sunyaev 1975, 1976)[2]

[2] We define $Q = Q_x 10^x$ in cgs units if not mentioned otherwise.

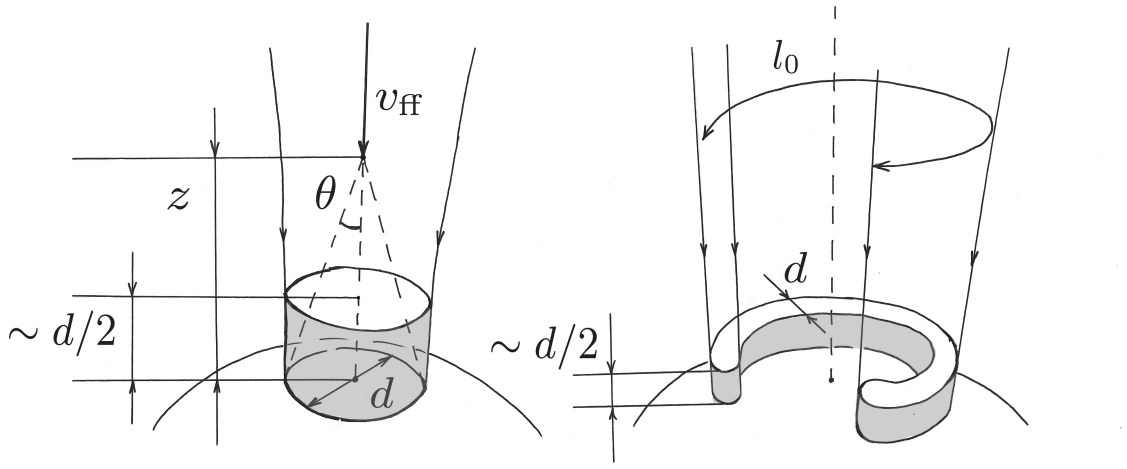

Figure 1. The infalling matter is decelerated by the radiation pressure force from the hotspot. Photons are coming from the hotspot within the solid angle, which is defined by the distance of a given point from the surface.Accretion via the wind (left) and the disc (right) leads to a different geometry of the accretion channel and the hotspot shape, as well to the different structure of the braking region. In any case the effective deceleration $g_{\rm R}$ drops rapidly with the distance from the surface z and the radiation pressure decelerates the infalling matter effectively only in the layer $0 < z \lesssim d/2$ (Basko & Sunyaev 1975; Lyubarskii & Syunyaev 1982).

$$L^* \approx \frac{c}{\kappa_{\rm eff}} \pi d \frac{GM}{R} \approx 3.7 \times 10^{36} \left(\frac{\kappa_{\rm T}}{\kappa_{\rm eff}}\right) \frac{d_5}{R_6} m \text{ erg s}^{-1}, \qquad (7)$$

where $\kappa_{\rm T} \approx 0.34$ cm^2 g^{-1} is the Thomson scattering opacity for solar composition material and $m = M/{\rm M}_\odot$.

If accretion to the NS with dipole magnetic field proceeds through the accretion disc, the matter is confined to a narrow wall of magnetic funnel and the hotspots have a shape of ring with a base length l_0 and width d instead of circles (Fig. 1). The estimation for the critical luminosity (7) is also valid for this case if we replace $\pi d \to l_0$ (Basko & Sunyaev 1975, 1976).

The approach described presented above assumes that all kinetic energy of the infalling matter is spent to heat the NS surface and accounts only for radiation from the hotspots. A realistic physical picture is more complicated:

(i) scattering on the infalling electrons is incoherent, so that the photons get a fraction of the electron momentum and energy;

(ii) photons are scattered predominantly downwards heating the NS surface even more, and

(iii) a fraction of them are scattered back towards the infalling matter and gets more energy and momentum.

As a result of this bulk Comptonization process (Blandford & Payne 1981a), a radiation-dominated shock is formed (Zel'dovich & Raizer 1967; Blandford & Payne 1981b), where matter is heated up and is decelerated from the supersonic infall velocity to the sub-sonic sedimentation velocity. The observed power-law-like spectra of XRPs also could be formed due to the bulk Comptonization in the radiation-dominated shock (Lyubarskii & Syunyaev 1982; Becker & Wolff 2007). The optical depth of the radiation-dominated shock is about $\tau \sim 5 - 7$ (Zel'dovich & Raizer 1967), and thus the considered above deceleration slab is optically thick (see next section). Therefore, it is necessary to consider the radiation transfer accounting for thermal and bulk Comptonization and the dynamics of the infalling plasma self-consistently. However, we expect that most of these complications are of little importance while the major effects are coming from the energy dependence of the effective opacity which may change by orders of magnitude. Thus we assume that equation (7) is a good first approximation.

The critical luminosity is defined by the mass and the radius of a star, geometry of the accretion flow near the surface and the effective opacity. Interestingly, there is no explicit dependence of the critical luminosity on the thickness of the accretion channel. The effective opacity is determined by an effective cross section $\sigma_{\rm eff}$:

$$\kappa_{\rm eff} = \frac{\sigma_{\rm eff}}{\mu_{\rm e}\, m_{\rm p}}, \qquad (8)$$

where $\mu_{\rm e} \approx 1.18$ is the mean molecular weight per free electron for the fully ionized plasma with the solar hydrogen-helium mixture.

The calculation of the effective cross-section is a key problem here. In a general case of magnetized plasma, its value is determined mainly by Compton scattering and cyclotron absorption (Harding & Lai 2006). However, we are interested in NSs with very strong B-field ($\gtrsim 10^{12}$ G). In such a fields the cyclotron decay rate is quite high and an electron that absorbs a cyclotron photon will be almost always de-excited by emitting another photon, rather than be collisionally de-exited. As a result the resonant scattering dominates over the true absorption (Bonazzola, Heyvaerts, & Puget 1979; Herold et al. 1982) and the principal process in the interaction is Compton scattering.

Compton scattering cross-section for high B-field depends strongly on photon energy (Daugherty & Harding 1986), with large variations around the cyclotron harmonics. Thus, photons of different energies make very different contribution to the radiation pressure force. Because in our calculations we do not compute the radiative transfer and the hotspot spectra self-consistently, we adopt a simple pre-

scription for the photon spectrum that is fully determined by the effective temperature $T_{\rm eff}$:

$$\sigma_{\rm SB} T_{\rm eff}^4 = F^*, \tag{9}$$

where $\sigma_{\rm SB}$ is the Stefan-Boltzmann constant.

It should be noted that the luminosity and the temperature are given here in the NS reference frame and corresponding corrections for the observed luminosity, $L^\infty = (1-u)L$, and the cyclotron energy, $E^\infty_{\rm cycl} = (1-u)^{1/2} E_{\rm cycl}$, have to be made if one wants to compare simulations with the data.

3 HOTSPOT AREA AND EFFECTIVE TEMPERATURE

The shape and the area of the hotspots are determined by the structure of the accretion channel. The spot area is defined mainly by the interaction between the NS magnetosphere and matter in the binary system. If a pulsar is fed from the accretion disc, the accretion flow in the vicinity of a NS has geometry of a narrow cylindrical ring. For the wind-fed pulsars, one can expect a completely filled funnel cavity. The magnetospheric radius depends on the B-field strength and structure, mass accretion rate and the way a pulsar is fed. It can be estimated with the following expression (Lamb, Pethick, & Pines 1973; Frank, King, & Raine 2002)

$$R_{\rm m} = 2.6\times10^8 \Lambda\, m^{1/7} R_6^{10/7} B_{12}^{4/7} L_{37}^{-2/7}\ {\rm cm}, \tag{10}$$

where Λ is a constant which depends on the accretion flow geometry: $\Lambda = 1$ for the case of spherical or wind accretion (W-case; for example, in Vela X-1), and $\Lambda < 1$ for the case of accretion through the disc (D-case; expected e.g. in Her X-1, GX 304–1, V 0332+53, 4U 0115+63), with $\Lambda = 0.5$ being a commonly used value (Ghosh & Lamb 1978, 1979). The W- and D-accretion scenarios give quite different predictions for the spot area because of the different structure of the accretion channel near the NS surface. At the same time we can consider these two scenarios as limiting cases because the accretion process in many system may partly proceed both ways.

In the W-case scenario, the hotspot area can be expressed as

$$\begin{aligned} S_W &\approx \pi d^2/4 \approx \pi R^3 R_{\rm m}^{-1} \\ &\approx 1.3\times10^{10}\,\Lambda^{-1}\, m^{-1/7}\, R_6^{11/7}\, B_{12}^{-4/7}\, L_{37}^{2/7} \quad {\rm cm}^2. \end{aligned} \tag{11}$$

under assumption of the dipole configuration of the B-field. Using equation (9) we then immediately get the effective temperature:

$$T_{\rm eff}^W = 4.5\,\Lambda^{1/4} B_{12}^{1/7}\, L_{37}^{5/28} m^{1/28}\, R_6^{-11/28} \quad {\rm keV}. \tag{12}$$

Expressions (11) and (12) give us the maximum hotspot area and, correspondingly, the minimum effective temperature for the fixed mass accretion rate.

In the D-case, matter comes closer to the NS (see equation (10)), the plasma is confined to a narrow wall of the magnetic funnel. The thickness of the accretion channel depends on the penetration depth of the accretion disc into the NS magnetosphere (Lai 2014), which is expected to be of the order of $\delta \approx 2H$, where H is a disc scale-height at the inner edge (Ghosh & Lamb 1978, 1979). We evaluate H using the Shakura & Sunyaev (1973) model, slightly modified how the vertical structure is averaged and using the correct Kramer opacity (Suleimanov, Lipunova, & Shakura 2007). The radius of magnetosphere for adopted parameters is situated in the so-called C-zone of accretion disc, where gas pressure and Kramer opacity dominate. The boundary of this zone for adopted parameters is situated at (Suleimanov et al. 2007)

$$r > r_{BC} \approx 5.5\times10^7\, L_{37}^{2/7}\, R_6^{2/7}\, m^{1/21} \quad {\rm cm}. \tag{13}$$

A relative disc scale-height at radius r for this zone is

$$\frac{H}{r} \approx 0.08\,\alpha^{-1/10}\, L_{37}^{3/20}\, m^{-21/40}\, R_6^{3/20}\, r_8^{1/8}, \tag{14}$$

where $\alpha < 1$ is a dimensionless viscosity parameter (Shakura & Sunyaev 1973). Substituting $R_{\rm m}$ from equation (10) to equation (14) instead of r, we get

$$\frac{H_{\rm m}}{R_{\rm m}} = 0.1\,\alpha^{-1/10}\,\Lambda^{1/8}\, m^{-71/140}\, R_6^{23/70}\, B_{12}^{1/14}\, L_{37}^{4/35}. \tag{15}$$

Then, the area of a single hotspot, which has a shape of a closed ring on the stellar surface, is

$$\begin{aligned} S_D &= l_0 d \approx 2\pi \frac{R^3}{R_{\rm m}} \frac{H_{\rm m}}{R_{\rm m}} \approx S_W \frac{2H_{\rm m}}{R_{\rm m}} \\ &\approx 3\times10^9\,\Lambda^{-7/8}\, m^{-13/20}\, R_6^{19/10}\, B_{12}^{-1/2}\, L_{37}^{2/5} \quad {\rm cm}^2. \end{aligned} \tag{16}$$

The corresponding effective temperature is

$$T_{\rm eff}^D = 6.6\,\Lambda^{7/32}\, m^{13/80}\, R_6^{-19/40}\, B_{12}^{1/8}\, L_{37}^{3/20} \quad {\rm keV}. \tag{17}$$

It is interesting that the obtained $T_{\rm eff}^D$ is close to the temperature of the hot electrons $T_{\rm e} \approx 5.1$ keV, when the observed spectrum of X-ray pulsar GX 301–2 was fitted by COMPTT model (Doroshenko et al. 2010).

If the magnetic dipole is inclined with respect to the orbital plane, the expressions for the hotspot areas would be different because the spot would have a shape of an open ring. It is reasonable then to use an additional parameter l_0/l, which shows what part of the full ring length l is exposed to accretion. We use this parameter further and analyse its influence on the final results.

3.1 Thomson optical thickness

The infalling plasma is stopped by the radiation force at the distance which is comparable to the thickness of the accretion channel d (Basko & Sunyaev 1976). Under the assumption of linear velocity decrease to zero value over the braking distance, the Thomson optical thickness of this layer is

$$\begin{aligned} \tau_{\rm T} \quad &\gtrsim \quad \kappa_{\rm T} \frac{\dot M}{2 S_D\, v_{\rm ff}}\, d \approx \kappa_{\rm T} \frac{\dot M}{4\pi r_0\, v_{\rm ff}} \\ &\approx 5\,\Lambda^{1/2}\, L_{37}^{6/7}\, B_{12}^{2/7}\, m^{-10/7}\, R_6^{10/14}, \end{aligned} \tag{18}$$

where $\dot M \approx 1.3\times10^{17}\, L_{37}\, m^{-1}\, R_6$ g s^{-1} is the mass accretion rate. Thus, the plasma is optically thick for the luminosity and the range of magnetic field strengths which are of interest here. The actual optical depth can be much smaller than $\tau_{\rm T}$ in the case of ultra-strong magnetic field, when photon energies are far below the cyclotron energy and the scattering cross-section is quite small. On the other hand, it can

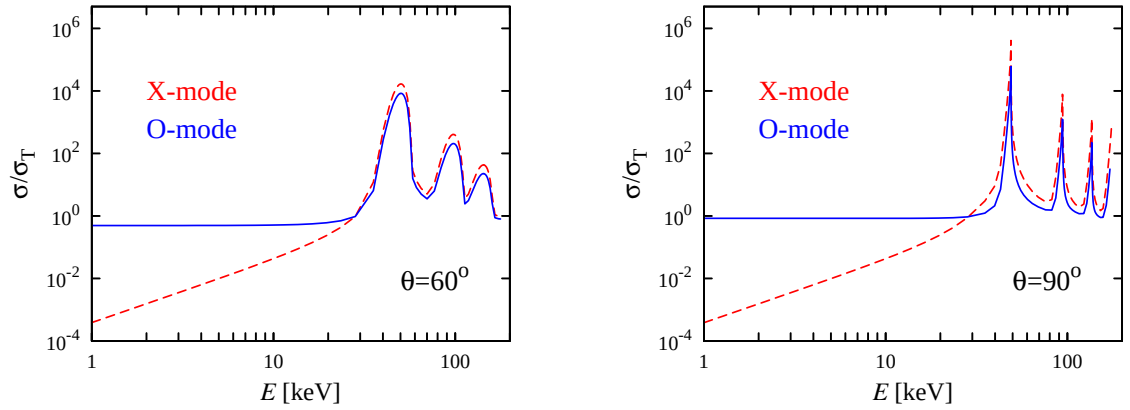

Figure 2. Total Compton scattering cross-section dependence on photon energy, polarization state (for X- and O-modes) and and the angle θ between the initial momentum direction and the B-field. The resonant features are broadened due to thermal motion of the electrons. Their positions depend on θ. Here the magnetic field strength is $b = 0.1$ (i.e. $B_{12} \simeq 4.4$) and the electron temperature $T_{\rm e} = 5$ keV.

be much larger than $\tau_{\rm T}$ if cyclotron resonances occur close to the peak of the spectral energy distribution.

4 COMPTON SCATTERING CROSS-SECTION

4.1 Calculations of Compton scattering cross-section

The cross-section of Compton scattering in strong magnetic field differs substantially from the cross-section of this process in low B-field. It depends strongly on the photon energy E, polarization mode j ($j = 1$ for the extraordinary mode – "X-mode", and $j = 2$ for the ordinary mode – "O-mode"), the angle θ between the B-field direction and the photon momentum, the strength of the B-field and the electron temperature $T_{\rm e}$. Resonances in the photon-electron interaction lead to extremely high values of the cross-section around the cyclotron frequency and its harmonics (Fig. 2). The exact positions of the resonances depend on the field strength and on the photon momentum direction:

$$\frac{E^{(n)}_{\rm res}(B)}{m_{\rm e}c^2} = \begin{cases} \dfrac{\sqrt{1+2nb\sin^2\theta}-1}{\sin^2\theta}, & \text{for } \theta \neq 0,\ n = 1, 2, ..., \\ b, & \text{for } \theta = 0, \end{cases} \quad (19)$$

where $b \equiv B/B_{\rm cr}$ is the B-field strength in units of the critical field strength $B_{\rm cr} = m_{\rm e}^2c^3/e\hbar = 4.412 \times 10^{13}$ G and $m_{\rm e}$ is the electron mass.

We calculate Compton scattering cross-section using the second order perturbation theory in quantum electrodynamics. Such calculations were already done by Pavlov, Shibanov & Iakovlev (1980), Daugherty & Harding (1986) and Harding & Daugherty (1991) (see A. Mushtukov et al., in prep., for the details) and the formalism was discussed partly by Mushtukov et al. (2012). The electron temperature $T_{\rm e}$ noticeably affects the cross-section near the resonance energies by thermal broadening of the peaks. Because electrons in strong B-field move mostly along the field lines, the broadening depends also on the angle between photon momentum and the field direction. Thermal broadening has its maximum for the photons which propagate along the field and minimum for photons moving in the perpendicular direction because only the relativistic transverse Doppler effect operates in this case. The scattering cross-section by an ensemble of electrons described by the distribution function over the longitudinal momentum $f(Z, T_{\rm e})$ (normalized to unity $\int_{-\infty}^{\infty} f(Z, T_{\rm e}){\rm d}Z = 1$) is (Harding & Daugherty 1991):

$$\sigma(E, \mu, T_{\rm e}) = \int\limits_{-\infty}^{\infty} {\rm d}Z\, f(Z, T_{\rm e})\sigma_{\rm R}(E_{\rm R}, \mu_{\rm R})\ \gamma(1 - \beta\mu), \quad (20)$$

where $\sigma_{\rm R}(E_{\rm R}, \mu_{\rm R})$ is the cross-section for electrons at rest (indicated by subscript R). Here $\mu = \cos\theta$ and $\mu_{\rm R}$ are related by the relativistic aberration formula, $\beta = v/c$ is dimensionless electron velocity corresponding to the dimensionless electron momentum $Z = \beta\gamma$ and $\gamma = (1 - \beta^2)^{-1/2}$ is the Lorentz factor.

A good lower estimate for the electron temperature $T_{\rm e}$ of the accretion flow comes from the fact that for luminous pulsars X-ray radiation keeps the gas at the Compton temperature. For a typical XRP spectrum with photon index $\Gamma \approx$ 1–1.5 and a cutoff at 20–30 keV, the Compton temperature lies in the interval 1–5 keV. The upper limit on the temperature comes from the cutoff energy and gives $T_{\rm e} \sim 10$ keV. In further calculations we assume $T_{\rm e} = 1$ keV and discuss the effects of possible deviation from that value.

4.2 Effective cross-section

The effective cross-section defines the radiation pressure, and, hence, the critical luminosity for a given magnetic field strength. It depends on the photons distribution over energy, directions of propagation and polarization states.

The expression for radiation force could be written in the following way (see e.g. equation (2.50) in Pozdnyakov, Sobol & Syunyaev 1983):

$$g_{\rm R} = \frac{1}{c}\sum_{j,n_{\rm f}}\int\limits_0^{\infty}{\rm d}E_{\rm i}\int\limits_{(4\pi)}{\rm d}\Omega_{\rm i}\int\limits_0^{\infty}{\rm d}E_{\rm f}\int\limits_{(4\pi)}{\rm d}\Omega_{\rm f} \quad (21)$$
$$\times\ \frac{{\rm d}\sigma_j(E_{\rm i}, \mu_{\rm i}|E_{\rm f}, \mu_{\rm f}, n_{\rm f}, T_{\rm e})}{{\rm d}E_{\rm f}{\rm d}\Omega_{\rm f}} I_j(E_{\rm i}, \mu_{\rm i})\left(\mu_{\rm i} - \frac{E_{\rm f}}{E_{\rm i}}\mu_{\rm f}\right),$$

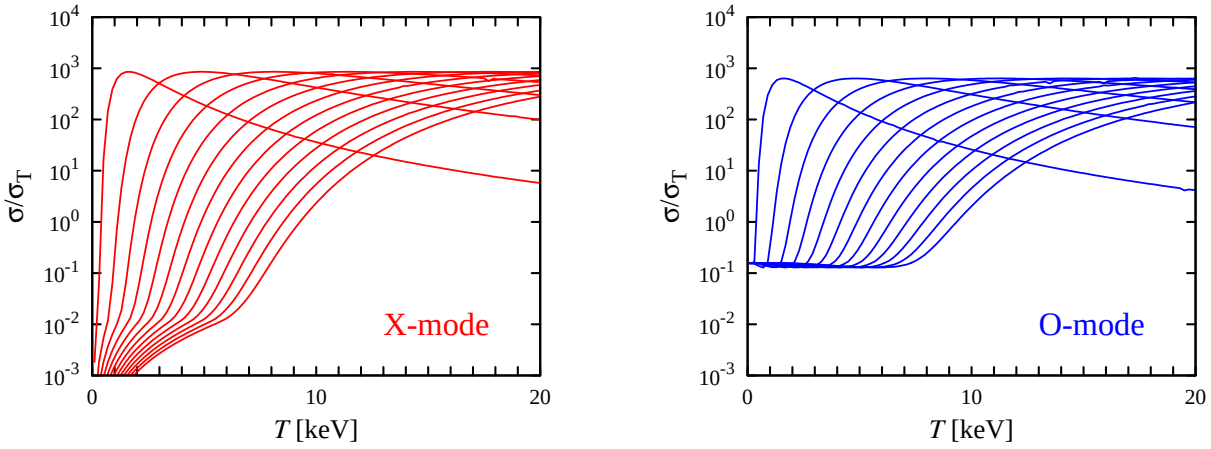

Figure 3. The mean cross-section for photons of X- and O- polarization modes as a function of the blackbody temperature (see equation (25)). The different lines correspond to various magnetic field strength starting from $b = 0.02$ up to $b = 0.5$ with a step $\Delta b = 0.04$ (from left to right). The electron temperature is fixed at $T_{\rm e} = 1$ keV.

where $\mathrm{d}\sigma_j/\mathrm{d}E_{\rm f}\mathrm{d}\Omega_{\rm f}$ is the differential cross section, indexes "i" and "f" denote the initial and final particle conditions, $I_j(E_{\rm i},\mu_{\rm i})$ is the intensity corresponding to a given photon polarization state j (X- or O-mode), energy $E_{\rm i}$ and direction $\mu_{\rm i}$. The difference $(\mu_{\rm i} - \mu_{\rm f}E_{\rm f}/E_{\rm i})$ defines the recoil effect in each scattering event. The summation is made over the final Landau level numbers $n_{\rm f}$ and photon polarization states j. The total scattering cross section for a given polarization state is

$$\sigma_j(E_{\rm i},\mu_{\rm i},T_{\rm e}) = \sum_{n_{\rm f}} \int_0^\infty \mathrm{d}E_{\rm f} \int_{(4\pi)} \mathrm{d}\Omega_{\rm f} \frac{\mathrm{d}\sigma_j(E_{\rm i},\mu_{\rm i}|E_{\rm f},\mu_{\rm f},n_{\rm f},T_{\rm e})}{\mathrm{d}E_{\rm f}\mathrm{d}\Omega_{\rm f}}. \quad (22)$$

If the photon redistribution is symmetric relative to the plane perpendicular to the initial photon momentum (it is a reasonable assumption for the relatively low-energy photons $E \ll m_{\rm e}c^2$), then each photon on average transfer its own momentum to the electron and the expression for the radiation force (21) can be simplified:

$$g_{\rm R} = \frac{1}{c}\sum_j \int_0^\infty \mathrm{d}E \int_{(2\pi)} \mathrm{d}\Omega\ \sigma_j(E,\mu,T_{\rm e})\ I_j(E,\mu)\ \mu. \quad (23)$$

In the following we use this simplified expression because photons emitted from the hotspots are not expected to have energies higher than ~ 20 keV.

For optically thin plasma falling onto the NS surface, the hotspot radiation spectrum does not change and the expression for the radiation force in the plasma reference frame takes the form

$$g_{\rm R} \approx \frac{\pi}{c}\sum_j \int_0^\infty \mathrm{d}E \int_{\mu^*}^1 \mathrm{d}\mu\,\mu\ \sigma_j(E,\mu,T_{\rm e})\ B_{\rm E}(T(\mu)), \quad (24)$$

where $B_{\rm E}(T)$ is the Planck function, $T(\mu) = T_{\rm eff}\gamma(1+\beta\mu)$ and $\mu^* = (\mu_0+\beta)/(1+\beta\mu_0)$, μ_0 is cosine of the maximum polar angle from which spot radiation is coming. Equation (24) is written for the axisymmetric case assuming blackbody radiation. The light aberration and the transformation of the radiation field due to the Lorentz transformation are taken into account. Because by definition $g_{\rm R} = \sigma_{\rm eff}F/c$, the effective cross section in this case is

$$\sigma^{(1)}_{\rm eff} = \frac{\sum_j \int_0^\infty \mathrm{d}E \int_{\mu^*}^1 \mathrm{d}\mu\,\mu\ \sigma_j(E,\mu,T_{\rm e})\ B_{\rm E}(T(\mu))}{\sum_j \int_0^\infty \mathrm{d}E \int_0^1 \mathrm{d}\mu\,\mu\ B_{\rm E}(T_{\rm eff})}. \quad (25)$$

The results of calculations are shown in Fig. 3.

On the other hand, in the case of the optically thick plasma, the radiation field could be modified significantly and the situation is much more complicated. In general, it is necessary to calculate accurately the radiation transfer problem together with the structure of a radiation-dominated shock near the surface. However, it is also possible to get the approximate effective cross-section using the Rosseland approximation (van Putten et al. 2013). For the angle-independent cross-section, the Rosseland mean value has a well known form

$$\frac{1}{\sigma_R} = \frac{\int_0^\infty \frac{\mathrm{d}B_E(T)}{\mathrm{d}T}\frac{1}{\sigma(E)}\mathrm{d}E}{\int_0^\infty \frac{\mathrm{d}B_{\rm E}(T)}{\mathrm{d}T}\mathrm{d}E}. \quad (26)$$

For the angle-dependent cross-section the expression can be generalized:

$$\frac{1}{\overline{\sigma}_j} = \frac{\int_0^\infty \frac{\mathrm{d}B_{\rm E}(T)}{\mathrm{d}T}\mathrm{d}E \int_0^1 \mathrm{d}\mu\,3\mu^2\frac{1}{\sigma_j(E,\mu,T_{\rm e})}}{\int_0^\infty \frac{\mathrm{d}B_{\rm E}(T)}{\mathrm{d}T}\mathrm{d}E}. \quad (27)$$

The Rosseland cross-section as a function of the B-field strength and the temperature is shown in Fig. 4 for both polarizations. We note that the cross section is significantly smaller than that for the optically thin case.

The hotspot radiation is interacting with the moving plasma inside the radiation shock region and braking it. The spectra in the star reference frame and in the moving electron reference frame are different due to the Doppler shift and relativistic aberration. Moreover the interaction

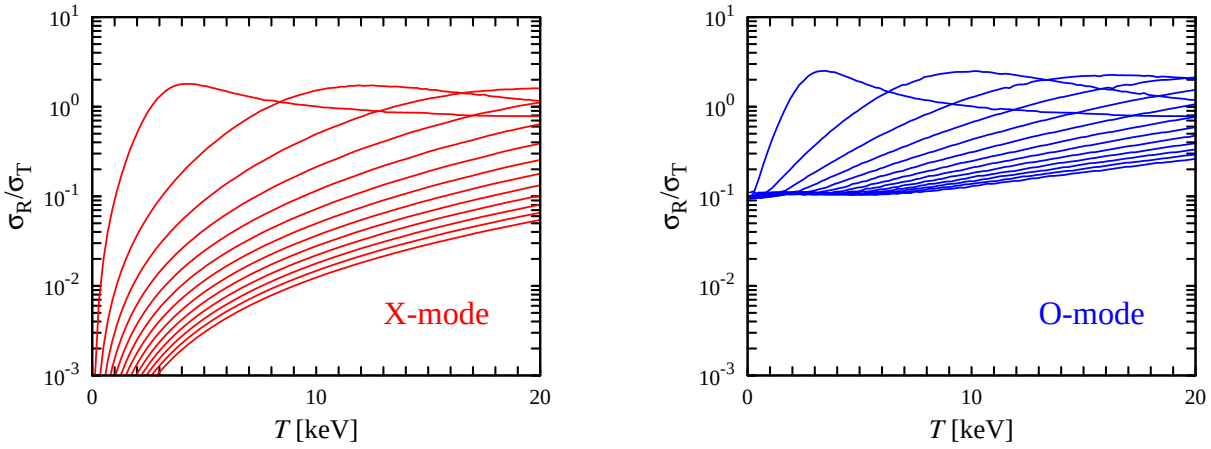

Figure 4. The Rosseland mean cross-section for photons of X- and O- polarization modes as a function of the blackbody temperature. The different lines correspond to various magnetic field strength starting from $b = 0.02$ up to $b = 0.5$ with a step $\Delta b = 0.04$ (from left to right). The electron temperature is fixed at $T_e = 1$ keV.

between infalling plasma and the hotspot radiation changes the spectrum. As a result the characteristic photon energy is a bit higher than it is expected from the obtained effective temperature (Section 3). The problem could be solved approximately with the correction of the effective temperature in equation (27). Under the assumption of free photon escape from the accretion channel walls and free supersonic gas infall down to the shock front, the velocity profile inside the shock region is $v(z) = v_{\rm ff}(1-\exp[-z/d])$, where z is the height of a given point (Lyubarskii & Syunyaev 1982). The photon energy shift in the electron reference frame depends on the electron velocity and the angle between photon and electron momenta. Taking into account the electron velocity profile in the shock region and distribution of photons over momentum direction we estimate that the radiation temperature in the plasma frame is larger than the effective temperature by a factor $1 < \zeta \lesssim 1.5$, i.e. we should use $T = \zeta T_{\rm eff}$ in equation (27). The initial hot spot spectrum is not well known and might differ from the blackbody spectrum. The corresponding measure of the mean photon energy is corrected by a factor of 0.5–1, with the lower value corresponding to the bremsstrahlung and the upper value to the Planck spectrum. This difference can be also taken into account by ζ-coefficient. In our primary calculations we use $\zeta = 1.5$ and discuss an influence of the coefficient on the final results in Section 5.1.

Rosseland mean value (27) is written for the case of fixed photon polarization state. In the case of mixed polarization the effective cross-section can be expressed as

$$1/\sigma^{(2)}_{\rm eff} = \eta/\overline{\sigma}_1 + (1-\eta)/\overline{\sigma}_2, \qquad (28)$$

where η is a fraction of radiation in the X-mode. This equation is written under assumption that the photon fraction of each polarization does not depend on photon energy. In reality the problem could be more complicated and it can be a function of photon energy and even of direction, but for the simple estimations it is reasonable to assume that photons of different polarizations are mixed in some proportion. We use η as a parameter in our calculations. Because the optical depth of the shock is large (see equation (18)), it makes more sense to use the Rosseland mean opacity for calculation of the critical luminosity.

5 RESULTS

5.1 Critical luminosity

The main parameters defining the effective cross-section are the magnetic field strength (i.e. cyclotron energy $E_{\rm cycl}$), the effective temperature $T_{\rm eff}$ and the polarization mixture η. Once the effective (Rosseland) cross-section is obtained, we can compute the critical luminosity. The results obviously depend on the radiation field structure. In order to estimate the critical luminosity approximately we assume the blackbody spectrum with the effective temperature which is defined by the mass accretion rate and the hotspot area (see Section 3). The critical luminosity also depends on the NS mass and radius and accretion flow geometry. The expression for the critical luminosity is not linear: the effective cross section in the right hand side of equation (7) is defined by the effective temperature and therefore by the hot spot area, which depends on the mass accretion rate or luminosity. Thus, the expression for the luminosity could not be used directly. We solve the problem in an iterative way. We start with fixed magnetic field strength and some reasonable luminosity value ($L_{37} = 1$). They give us the spot area and the effective cross section. Then we compute new luminosity value using equation (7) which gives the new effective cross section. This procedure continues until the difference between new and previous luminosities is sufficiently small. In the end we have self-consistent values for the critical luminosity and the effective cross section for a given B-field strength.

Let us first demonstrate why it is important to compute Compton scattering cross-section accurately in order to get the correct behaviour of the critical luminosity on the B-field strength. For Thomson cross-section, the dependence is monotonic (see dotted black curve in Fig. 5a) and just reflects the fact that at higher B the spot area becomes smaller. The effect of the resonances can be demonstrated if we ignore them and take the cross section in the following

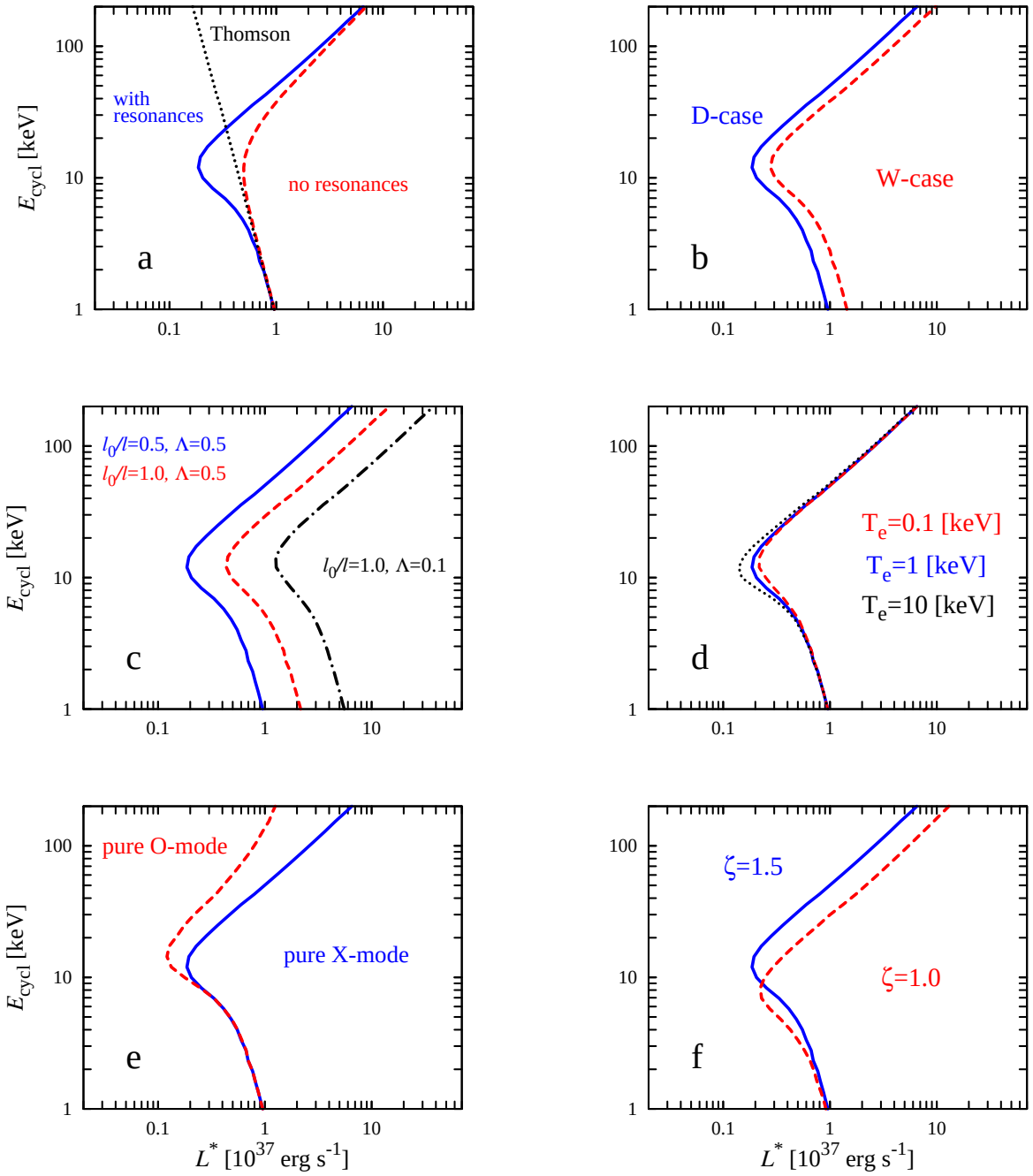

Figure 5. Dependence of the critical luminosity on the magnetic field strength expressed as an inverse relation of the cyclotron energy on luminosity. The fiducial case is given by solid blue line and corresponds to disc-case with the following set of parameters: $m = 1.4$, $R_6 = 1$, $l_0/l = 0.5$, $\Lambda = 0.5$, $T_e = 1$ keV, $\zeta = 1.5$, pure X-mode polarization is also assumed. (a) The effect of the resonant scattering and deviation of the cross-section from the Thomson value. At low B (i.e. low cyclotron energies), the critical luminosity is similar to that for Thomson cross-section (shown by black dotted line). Resonances reduce the critical luminosity, when the cyclotron line energy is close to the typical photon energy from the hotspot. (b) Dependence on the accretion flow structure. The wind case predicts slightly higher critical luminosity, mostly because of the larger hotspot size that leads to smaller temperature and larger breaking distance. (c) Influence of the geometry of the accretion channel and the size of the magnetospheric radius. (d) Electron temperature in the accretion flow affects the resonance width and is important only for the case when most of the photons come inside of the resonance. (e) Dependence on polarisation. In high magnetic field the scattering cross-section for different photon polarizations is vastly different. (f) Effects of effective temperature change due to the motion of optically thick plasma.

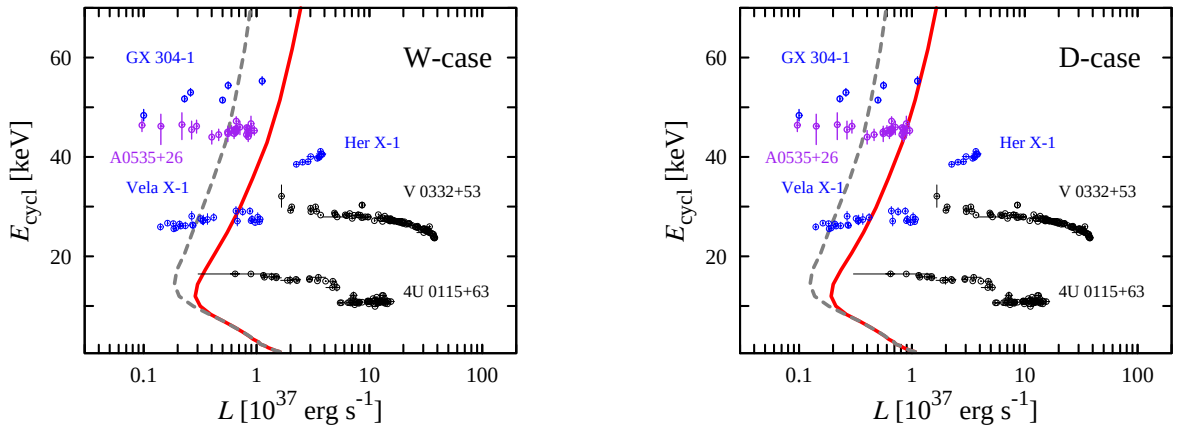

Figure 6. Comparison of the theoretical critical luminosity–$E_{\rm cycl}$ dependence to the data. In the W-case (left): matter fills the whole funnel cavity, while in the D-case (right) matter is confined a narrow wall of magnetic funnel. We use $\Lambda = 0.5$ and $l_0/l = 0.5$ to define the accretion channel geometry in the D-case. The grey and red curves show the theoretical dependences for pure O- and X-mode polarizations, respectively. The data are plotted by blue circles for pulsars which show subcritical luminosity behaviour and by black circles for pulsars which supercritical behaviour. For Vela X-1, the energy of the first harmonic divided by two is used. Other parameters are $M = 1.4{\rm M}_\odot$, $R = 10^6$ cm, $T_{\rm e} = 1$ keV.

form (Basko & Sunyaev 1975):

$$\begin{aligned}
\sigma_{\rm X} &= \sigma_{\rm T}\left(\frac{E}{E_{\rm cycl}}\right)^2, && E < E_{\rm cycl},\\
\sigma_{\rm O} &= \sigma_{\rm T}\left(\sin^2\theta + \left(\frac{E}{E_{\rm cycl}}\right)^2\right), && E < E_{\rm cycl},\\
\sigma_{\rm X} &= \sigma_{\rm O} = \sigma_{\rm T}, && E \geq E_{\rm cycl}.
\end{aligned} \qquad (29)$$

The solid blue and the red dashed curves in Fig. 5(a) show the dependences of the critical luminosity on B computed with resonances and without them. We see that the dependence without resonances is much smoother. At small as well as large B, the curves coincide, just because most of the photons here come outside of the resonances. However, as soon as $kT_{\rm eff} \approx E_{\rm cycl}$, resonances increase the effective cross-section and reduce thus the critical luminosity.

Accretion flow geometry is a source of principal uncertainties. It affects the shape of the hot spot, its effective temperature and thereby defines the effective cross section. The critical luminosities for the W- and D-cases are compared in Fig. 5(b). We see that qualitatively the behaviour is very similar. The effect of the pulsar inclination reflected in different length of the annular arc l_0 is shown in Fig. 5(c). The temperature of the plasma influences the depth of the dip in the critical luminosity around $E_{\rm cycl} \sim 10$ keV (see Fig. 5d) affecting the width the resonance. Similarly, the correction to the effective temperature ζ because of the high plasma velocity shifts the resonance position and changes slightly the shape of the curve (see Fig. 5f). The effect of polarization is very strong at high B (see Fig. 5e) because of the very different behaviour of the cross-section of the X- and O-mode below the first resonance (se equation (29)). At low B the cross-sections above the resonance are similar and therefore the critical luminosities coincide. In reality the polarization composition could be a function of the photon energy and the optical depth of a given point (Miller 1995).

Our main conclusion that comes from Fig. 5 is that the behaviour of the critical luminosity on the B-field strength is very robust. It has a minimum of a few times 10^{36}erg s^{-1} for $E_{\rm cycl} \sim$10–20 keV and increases to $\sim 10^{37}$erg s^{-1} for low B nearly independent of the parameters. For the X-mode, the critical luminosities increases sharply towards large B owning to the drop of the Compton scattering cross-section below the resonance, while the increase is less dramatic for the O-mode.

5.2 Comparison with the data

For a given set of parameters we are able to calculate the critical luminosity as a function of the B-field strength (or, alternatively, of the cyclotron energy). As was discussed in the Introduction, the obtained dependence should separate the sources with hotspots on the NS surface from the sources with accretion columns. Therefore, it is expected that the sources with luminosities to the left from the curve show a positive correlation between cyclotron line centroid energy and luminosity while the sources with luminosities to the right should show a negative correlation.

In order to verify our theoretical predictions we use the observations of five X-ray pulsars for which the dependence of cyclotron energy (or first harmonic energy as it is for Vela X-1) on luminosity is firmly established: GX 304–1 (Klochkov et al. 2012), Her X-1 (Staubert et al. 2007; Vasco, Klochkov, & Staubert 2011), V 0332+53 (Tsygankov et al. 2010), 4U 0115+63 (Tsygankov et al. 2007), A 0535+26 (Caballero et al. 2007) and Vela X-1 (Fürst et al. 2014). It is believed that in all sources except Vela X-1 the mass accretion occurs mainly through the disc. Vela X-1 belongs to systems where accretion process occurs through the wind. It is also an exceptional case since a clear increase of the first harmonic energy with luminosity is visible, while the evolution of the energy of fundamental line with the luminosity is difficult to interpret. Thus, for Vela X-1 we use the energy of the harmonic divided by two on the plots.

Two sources – V 0332+53 with a confident negative correlation (Tsygankov et al. 2010) and 4U 0115+63 with

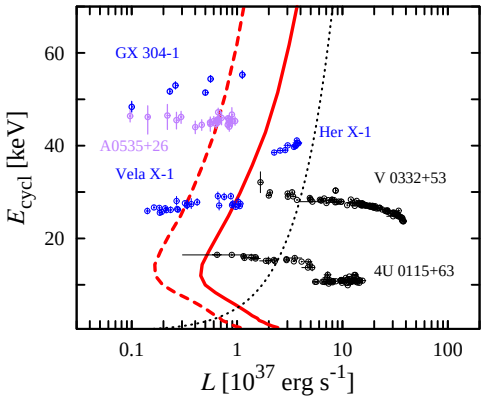

Figure 7. Red solid and dashed curves corresponds to the disc-accretion case with different parameters. The dashed curves is for $l_0/l = 0.5$ and mixed polarization (the flux in X- and O-modes are equal), while the solid curve is for $l_0/l = 1.0$ and pure X-mode polarization. In both cases $T_e = 1$ keV, $\Lambda = 0.5$ and $\zeta = 1.5$. The real critical luminosity value lies likely between the two curves. The predictions by Becker et al. (2012) are shown with the black dotted line. For the case of Vela X-1 the first harmonic energy divided by two is presented. Other parameters: $M = 1.4M_\odot$, $R = 10^6$ cm, $T_e = 1$ keV.

probable negative correlation (Tsygankov et al. 2007; Müller 2013; Boldin, Tsygankov, & Lutovinov 2013) – clearly belong to the area of supercritical accretion. One source, GX 304–1, which shows a positive correlation (Yamamoto et al. 2011; Klochkov et al. 2012), belongs to the area of subcritical accretion. The recent *NuSTAR* observations of Vela X-1 show some hints on the positive correlation between the position of first harmonic of the cyclotron line and luminosity (Fürst et al. 2014). It is likely that the critical luminosity of Vela X-1 is around 10^{37} erg s^{-1}. A 0535+26 which does not show positive or negative correlation (Caballero et al. 2007) also belongs to the area of subcritical accretion.

The theoretical critical luminosity versus observed cyclotron energy curves for the wind and the disc accretion cases are shown in Fig. 6 together with the data. We see that models well describe the data separating the two regimes, subcritical and supercritical, where the correlation changes from positive to the negative one. The X-mode polarization model is clearly preferred.

Her X-1, which probably shows a positive correlation (Staubert et al. 2007; Vasco et al. 2011), should belong to the region of subcritical accretion as well. It is slightly off our relation. The critical luminosity for Her X-1 seems a bit higher than the predicted one, possibly because of the strong non-dipole B-field component, which leads to a larger base area of the accretion channel (Shakura, Postnov, & Prokhorov 1991). Alternatively, the data on Her X-1 can be explained if we assume $\Lambda = 0.1$ as proposed by Becker et al. (2012). This would shift the critical luminosity curve to the right by a factor of ~ 2.5. Such a small Λ, however, contradicts theories of disc– magnetosphere interaction (see e.g. Ghosh & Lamb 1979; Lai 2014).

Fig. 7 demonstrates our theoretical curves for two possible polarization mixtures along with the data. We see that the model for pure X-mode describes the data better. For comparison we also show the prediction of the model by Becker et al. (2012) (black dotted curve) which contradicts the behaviour of V 0332+53 and 4U 0115+63.

6 SUMMARY

Following the theoretical model by Basko & Sunyaev (1975, 1976) we have calculated the critical luminosity for the magnetized NS as a function of magnetic field strength (or, equivalently, as a function of the cyclotron energy). For the first time the exact effective cross section for Compton scattering in a strong magnetic field (Daugherty & Harding 1986) including the resonances was used. We have investigated the dependence of the results on the polarization composition, the geometry of the accretion flow and the temperature of the accreting gas.

We showed that L^* is not a monotonic function of the field strength and reaches its minimal value of a few $\times 10^{36}$erg s^{-1} around the observed cyclotron energy $\sim$10 keV that corresponds to the surface magnetic field strength of $B \sim 10^{12}$ G. Such critical luminosity is reached when a considerable amount of photons from a hotspot have energy close to the cyclotron resonance and the effective cross section reaches its maximum. Since the typical hotspot temperature is a few keV, the critical luminosity reaches its minimum for the sources which have the cyclotron line close to the spectral peak. The critical luminosity increases for small B to $L^* \sim 10^{37}$erg s^{-1} nearly independent of the parameters. It also increases at large B-field strength because photons have much smaller cross section below the cyclotron energy. This behaviour is very robust and depends very little on the details of the model.

The obtained dependence of the critical luminosity on the B-field strength should separate sources in subcritical regime of accretion with a hotspot on the NS surface from supercritical regime with an accretion column. Therefore, we expect to observe a positive and a negative correlation between the cyclotron line centroid energy and the luminosity for the sources below and above the critical luminosity, respectively.

The comparison between the theoretical results and the data gives us an opportunity to obtain important parameters describing the accretion process onto a magnetised NS and provides additional method of diagnostics for systems with accreting NS. The expected appearance in the near future of the high quality data from the currently operating and planned X-ray telescopes will provide an excellent opportunity to verify the proposed theoretical predictions and to constrain some key parameters.

ACKNOWLEDGEMENTS

This research was supported by the Magnus Ehrnrooth Foundation (VFS and JP), the Jenny and Antti Wihuri Foundation (VFS and JP), the Russian Scientific Foundation grant 14-12-01287 (AAM), the Academy of Finland grant 268740 (JP), the German research Foundation (DFG) grant SFB/Transregio 7 "Gravitational Wave Astronomy" and the Russian Foundation of Fundamental Research grant 12-02-97006-r-povolzhe-a (VFS), the grant RFBR 12-02-

01265 (SST). We are grateful to Dmitrij Nagirner for a number of useful comments.

REFERENCES

Basko M. M., Sunyaev R. A., 1975, A&A, 42, 311
Basko M. M., Sunyaev R. A., 1976, MNRAS, 175, 395
Becker P. A. et al., 2012, A&A, 544, A123
Becker P. A., Wolff M. T., 2007, ApJ, 654, 435
Blandford R. D., Payne D. G., 1981a, MNRAS, 194, 1033
Blandford R. D., Payne D. G., 1981b, MNRAS, 194, 1041
Boldin P. A., Tsygankov S. S., Lutovinov A. A., 2013, Astr. Lett., 39, 375
Bonazzola S., Heyvaerts J., Puget J. L., 1979, A&A, 78, 53
Caballero I. et al., 2007, A&A, 465, L21
Caballero I., Wilms J., 2012, Mem. Soc. Astron. Italiana, 83, 230
Coburn W. et al., 2002, ApJ, 580, 394
Daugherty J. K., Harding A. K., 1986, ApJ, 309, 362
Doroshenko V., Santangelo A., Suleimanov V., Kreykenbohm I., Staubert R., Ferrigno C., Klochkov D., 2010, A&A, 515, A10
Filippova E. V., Tsygankov S. S., Lutovinov A. A., Sunyaev R. A., 2005, Astr. Lett., 31, 729
Frank J., King A., Raine D. J., 2002, Accretion Power in Astrophysics. Cambridge University Press, Cambridge
Fürst F. et al., 2014, ApJ, 780, 133
Ghosh P., Lamb F. K., 1978, ApJ, 223, L83
Ghosh P., Lamb F. K., 1979, ApJ, 232, 259
Gnedin I. N., Sunyaev R. A., 1974, A&A, 36, 379
Gnedin Y. N., Sunyaev R. A., 1973, MNRAS, 162, 53
Harding A. K., Daugherty J. K., 1991, ApJ, 374, 687
Harding A. K., Lai D., 2006, Rep. Prog. Phys., 69, 2631
Herold H., Ruder H., Wunner G., 1982, A&A, 115, 90
Klochkov D. et al., 2012, A&A, 542, L28
Lai D., 2014, EPJWC, 64, 1001
Lamb F. K., Pethick C. J., Pines D., 1973, ApJ, 184, 271
Lyubarskii Y. E., Syunyaev R. A., 1982, Sov. Astr. Lett., 8, 330
Mihara T., Makishima K., Nagase F., 2004, ApJ, 610, 390
Miller M. C., 1995, ApJ, 448, L29
Mitrofanov I. G., Pavlov G. G., 1982, MNRAS, 200, 1033
Mukherjee D., Bhattacharya D., Mignone A., 2013, MNRAS, 430, 1976
Müller S. et. al., 2013, A&A, 551, A6
Mushtukov A. A., Nagirner D. I., Poutanen J., 2012, Phys. Rev. D, 85, 103002
Nishimura O., 2014, ApJ, 781, 30
Pavlov G. G., Shibanov I. A., Iakovlev D. G., 1980, Ap&SS, 73, 33
Poutanen J., Mushtukov A. A., Suleimanov V. F., Tsygankov S. S., Nagirner D. I., Doroshenko V., Lutovinov A. A., 2013, ApJ, 777, 115
Pozdnyakov L. A., Sobol I. M., Syunyaev R. A., 1983, Astrophysics and Space Physics Reviews, 2, 189
Shakura N. I., Postnov K. A., Prokhorov M. E., 1991, Astr. Lett., 17, 803
Shakura N. I., Sunyaev R. A., 1973, A&A, 24, 337
Staubert R., Shakura N. I., Postnov K., Wilms J., Rothschild R. E., Coburn W., Rodina L., Klochkov D., 2007, A&A, 465, L25
Suleimanov V. F., Lipunova G. V., Shakura N. I., 2007, Astr. Rep., 51, 549
Tsygankov S. S., Lutovinov A. A., Churazov E. M., Sunyaev R. A., 2006, MNRAS, 371, 19
Tsygankov S. S., Lutovinov A. A., Churazov E. M., Sunyaev R. A., 2007, Astr. Lett., 33, 368
Tsygankov S. S., Lutovinov A. A., Serber A. V., 2010, MNRAS, 401, 1628
van Putten T., Watts A. L., D'Angelo C. R., Baring M. G., Kouveliotou C., 2013, MNRAS, 434, 1398
Vasco D., Klochkov D., Staubert R., 2011, A&A, 532, A99
Yamamoto T. et al., 2011, PASJ, 63, 751
Zel'dovich Y. B., Raizer Y. P., 1967, Physics of shock waves and high-temperature hydrodynamic phenomena. Academic Press, New York
Zel'dovich Y. B., Shakura N. I., 1969, Soviet Ast., 13, 175